Available online at www.sciencedirect.com

Chemical Engineering Research and Design

journal homepage: www.elsevier.com/locate/cherd

Design and characterization of a novel perfusion reactor for biopharmaceuticals production

Molly Tregidgo[1], *Marie Dorn*[1], *Ciara Lucas*, *Martina Micheletti*[*]

Advanced Centre for Biochemical Engineering, Department of Biochemical Engineering, University College London, UK

ARTICLE INFO

Article history:
Received 2 December 2022
Received in revised form 25 April 2023
Accepted 26 April 2023
Available online 28 April 2023

Keywords:
Process intensification
Mixing
Fluid flow
Stirred-tank reactor
Perfusion
Scale-down models

ABSTRACT

The demand for commercially valuable biopharmaceuticals able to treat different immunopathological diseases has accelerated in the last few decades. In recent years the industry has shifted the preferred mode of operation towards continuous strategies and has favoured the adoption of perfusion approaches for the cell culture step. In this mode successful perfusion process examples have reached up to 10-fold higher cell densities and product titres than fed-batch, while maintaining product quality at reduced costs. Perfusion processes are operated at high cell densities where cells are retained, while product and waste are continuously removed. This leads to different requirements in flow and mixing in comparison to lower cell density operations, potentially influencing the cellular production performance and therefore product quality. As the pharmaceutical industry is highly regulated, ensuring homogeneity in the bulk throughout the process is critical, while oxygen and mixing requirements of high cell density cultures must be continuously met. This paper presents the design and characterization of a novel 250 mL stirred tank reactor (STR) developed to work in perfusion mode. The results presented include the experimental measurement of the power consumption, the mixing analysis of the flow within the bioreactor which informs design consideration and scaling efforts and the biological data of the perfusion stage with an industrially relevant cell line producing an IgG monoclonal antibody. The characterization allows the operating window of the reactor to be established, resulting in increased productivity of intensified cultures.

1. Introduction

Over the last decade biopharmaceuticals such as monoclonal antibodies (mAbs) have emerged to be the main drug product developed and manufactured. Due to their high selectivity against a specific target and their frequent application as treatment for a variety of immunopathological conditions like cancer, the demand for biopharmaceuticals is accelerating (Croughan et al., 2015, Kesik-Brodacka, 2018, Konstantinov and Cooney, 2015). The majority of these products are made using mammalian cell lines, where efficient bioprocessing strategies are critical for industrial production (Tripathi and Shrivastava, 2019). In addition, the

Abbreviation: C_i, Spacing between impellers; D_i, impeller diameter; DO, dissolved oxygen; D_T, tank diameter; H_B, baffle height; HCD, high cell density; H_i, impeller off bottom clearance; H_L, liquid height; H_T, tank height; k_La, oxygen mass transfer coefficient; L_S, length sparger; mAb, monoclonal antibody; NaAlg, sodium alginate; RV d^{-1}, reactor volumes per day; STR, stirred tank reactor; t_M, mixing time; $t_M * N$, mixing number; VCC, viable cell concentration; V_W, working volume; W_B, baffle width

* Correspondence to: Advanced Centre for Biochemical Engineering, University College London, Bernard Katz Building, Gower Street, London WC1E 6BT, UK.
E-mail address: m.micheletti@ucl.ac.uk (M. Micheletti).

[1] Joint first authorship.

https://doi.org/10.1016/j.cherd.2023.04.066

biopharmaceutical industry is facing further challenges like growing competition of biosimilar products (Walsh, 2018), limitations in manufacturing capacity and requirements for product quality (Bielser et al., 2018, Rathore and Winkle, 2009). To tackle these, the industry is shifting towards continuous biomanufacturing, which for the cell culture stage means operating a bioreactor in perfusion mode, thus replacing the current state-of-the art fed-batch operation (Bielser et al., 2018, Mahal et al., 2021, Narayanan et al., 2022). The shift from a fed-batch to perfusion mode of operation aims at process intensification, reduction of product variability which results in improved product quality, and a decrease of production costs. (Arnold et al., 2019, Farid, 2019, Mahal et al., 2021, Narayanan et al., 2022).

The main feature of perfusion processes is the continuous removal of culture medium compensated by the continuous feed of fresh medium, while cells removed within the culture medium are captured by a cell retention device and returned to the bioreactor (Chotteau, 2015). The continuous medium renewal and cell retention enable the operation at high cell densities (HCD) as well as achieve higher productivities while maintaining product quality at reduced costs compared to an operation in fed-batch mode (Bielser et al., 2018, Chotteau, 2015). However, the medium exchange as well as the recirculation of cells back to the reactor might lead to variations in fluid flow and mixing. In addition, HCD cultures show changes of viscosity which must be considered given the impact viscosity has on the flow characteristics (Clincke et al., 2013a, Clincke et al., 2013b). For the operation at HCD, above the traditional concentration levels for fed-batch cultures, it is critically important to understand if a fluid becomes non-Newtonian during the process and at which cell densities. The change of viscosities could lead to variations in cellular production performance and product quality due to heterogeneities caused by slow mixing areas, thus influencing heat and mass transfer (Nienow, 1997, Nienow et al., 1996). Moreover, perfusion processes typically involve long process times and given the fact that the pharmaceutical industry is highly regulated, a deep and detailed understanding of the fluid flow within the bioreactor is critical and required to manage risk of failure. This is to ensure homogeneity throughout the process, while oxygen and mixing requirements of the HCD must be continuously met.

The increased complexity of a bioreactor in perfusion mode due to additional process parameter (e.g. flow rates) requires screening of multiple operating conditions to achieve high robustness and control. While for fed-batch operations microscale bioprocess techniques are well established, the same cannot be said for perfusion operations (Betts and Baganz, 2006). The development and optimisation of a perfusion bioprocess is associated with high costs and elongated time scales (Croughan et al., 2015), hence scale-down models represent an attractive tool to remain cost and time efficient as they facilitate high throughput optimisation by running multiple experiments in parallel (Bielser et al., 2018). Microbioreactor systems in sub-litre scales such as the ambr™ platform (Sartorius) or the DasBox system (Eppendorf) have been extensively studied and characterised for operations in fed-batch mode (Hsu et al., 2012, Nienow et al., 2013a), but comparable systems for perfusion culture are limited. Efforts have been made to establish methodologies that achieve cell retention through sedimentation, centrifugation or retrofitting of cell retention devices onto existing systems initially designed for fed-batch (Janoschek et al., 2019, Gagliardi et al., 2019, Jin et al., 2021, Sewell et al., 2019). Recently, the ambr250 platform (Sartorius) has been redesigned to fit perfusion requirements, where the recirculation is incorporated from the top of the bioreactor and a dual pitched-blade impeller system was implemented (Satorius, 2021). To the best of our knowledge, the design of a system at sub-litre scale tailored for perfusion operation aiming at optimising hydrodynamic conditions specific to HCD as well as a detailed characterisation regarding flow and mixing has not been performed until now. Perfusion processes are operated at HCD with significant oxygen demands, likely requiring the implementation of a dual impeller system to ensure efficient oxygen mass transfer while keeping the shear levels experience by the cells as low as possible.

This study presents the design and characterisation of a novel 250 mL stirred tank bioreactor operated in perfusion mode. This comprises design considerations and description of its geometry as well as characterisation of the vessel alongside recommendations for scaling criteria including k_La, mixing time and power input. Following this, the impact of perfusion-specific parameters such as the viscosity impact on the hydrodynamics of the system and the positioning of the re-circulation loop are discussed. Finally, a perfusion culture process is developed in the 250 mL bioreactor and performance is evaluated for both cell growth and productivity to demonstrate its validity for perfusion operations.

2. Material and methods

2.1. Design and fabrication of novel 250 mL bioreactor

The reactor vessel is designed to achieve a height (H_T) to diameter (D_T) ratio of approximately 1.5:1 (H_T:D_T) with H_T = 10 cm and D_T = 6.7 cm. The vessel bottom is flat, resulting in a liquid height of 7.4 cm (H_l/H_T = 0.74) for a working volume of 250 mL. Three baffles with a width of 0.5 cm and a height of 8 cm (H_b/D_T = 1.2) were incorporated in the vessel and evenly spaced with a spacing distance along the circumference of 7 cm between each. The system is stirred by two impellers, a top 3-blade pitched-blade impeller with a 30° pitch and a bottom 6-blade flat blade turbine impeller below (Eppendorf, Hamburg, Germany). Both impellers had an outer diameter of 3 cm (D_i/D_T = 0.44) and were internally spaced such that the off-bottom clearance was 0.33 D_T. The distance between the impellers was chosen to be equal to the impeller diameter, resulting in a spacing of C_i/D_T = 0.37. This ensures approximately equal spacing between the bottom, the two impellers and the top surface and avoids the top impeller to be located too close to the air interface. Further, the bioreactor was equipped with a L-shaped sparger for aeration with 7 drilled holes each with a diameter of 0.5 mm placed 0.5 cm (0.05 D_T) below the impeller. The headplate is designed as such that two elevated housings of 12 mm in diameter for pH and DO probe could be fitted within the vessel as well as additional ports for liquid addition and gas outlet. The electrolyte DO probe (OxyFerm; Hamilton) and pH probe (EasyFerm; Hamilton, NV, USA) had a diameter of 12 mm and a length of 12 cm. Additional ports with a diameter of 3.2 mm were placed in the base and the side of the vessel to connect to the cell retention device. The side port was placed at a height of 2.5 cm (0.37 D_T) from the bottom. Temperature was monitored using a thermowell temperature sensor (New Brunswick, Eppendorf) placed externally and assuming a

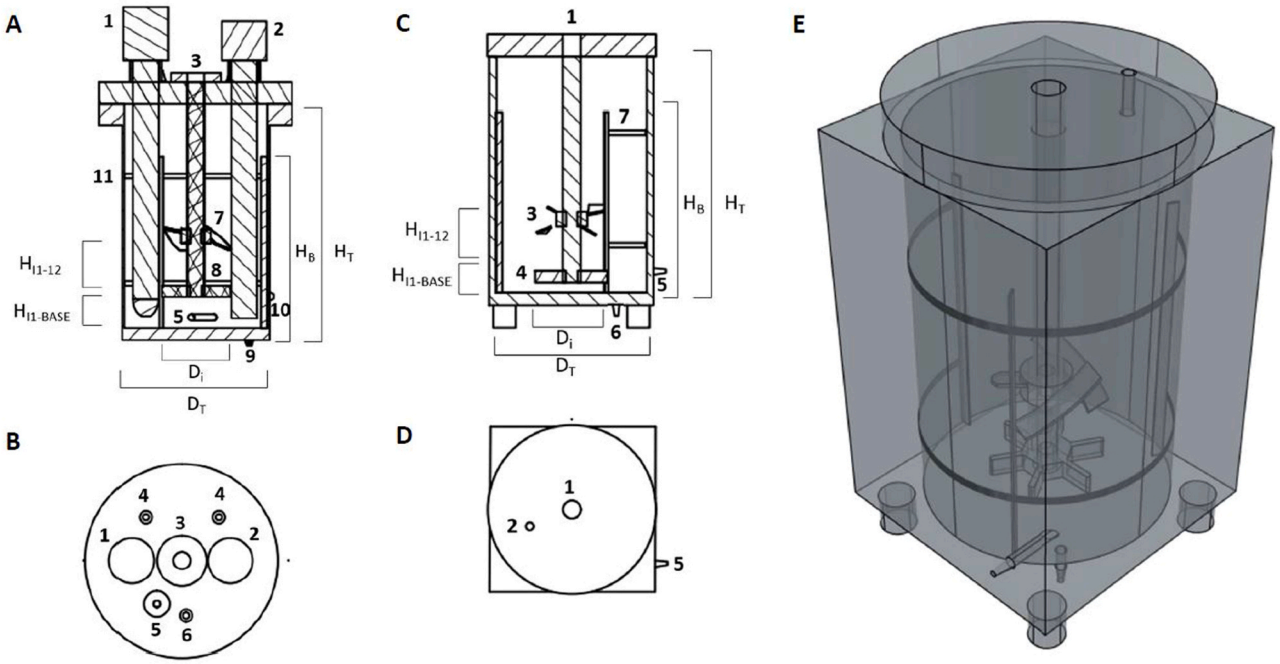

Fig. 1 – Design drawing and schematic diagrams of 250 mL novel bioreactor and acrylic mimic; (A) 2D cross section; (B) headplate; (C) 2D cross section of acrylic bioreactor mimic; (D) headplate of acrylic bioreactor mimic; (E) 3D view of acrylic mimic with X-ray allowing observations of internal components. Components of the 250 mL bioreactor: (1) pH probe port, (2) DO probe port, (3) impeller shaft, (4) liquid addition, (5) sparger, (6) gas outlet, (7) pitched blade impeller, (8) Rushton-style impeller, (9) connection to cell retention device – outlet, (10) connection to cell retention device – inlet, (11) baffles.

constant gradient of 3.5 °C between both sides of the tank wall.

A schematic diagram of the novel 250 mL bioreactor is presented in Fig. 1 A and B and was fabricated by the Design and Fabrication Facility at UCL using stainless-steel as base material which is sterilisable and therefore suitable for cell culture experiments. In addition, an acrylic mimic was fabricated to study engineering characteristics and observe internal bioreactor conditions. A schematic diagram and a 3D view of the acrylic mimic is shown in Fig. 1C-E. The acrylic mimic had identical internal dimensions as well as identical placements of the ports for recirculation on the side and bottom of the vessel. However, to increase the image quality taken in characterisation studies the mimic had flat external walls, as shown in Fig. 1E, reducing light refraction from the cylindrical surface of the mimic. It should be noted that the acrylic mimic in which engineering studies were conducted had no probe mimics, and as such the flow characteristics expected within the bioreactor would have been different from those measured experimentally within the mimic. The impact of type, geometry and number of probes on the power number in small scale reactors is currently the focus of ongoing studies and was not included in this work.

2.2. Viscosity measurements

For viscosity measurements, cells were expanded in a 1 L Erlenmeyer shake flask for 3 days. Following expansion, cells were centrifuged at 450 rpm for 5 min and re-suspended in fresh CD CHO medium at concentrations between 20 and 100×10^6 cells mL^{-1}. Measurements were performed using a rotational rheometer (Kinexus Lab+; Malvern Instruments, Malvern, UK) using a 1 mL sample at 37 °C, between 50 mm parallel plated with a 0.4 mm gap size. Viscosities were determined for an expected range of shear rates between 10 and 1000 s^{-1}. In addition to cell culture, viscosities of sodium alginate (NaAlg) solutions were measured in order to find a rheological transparent mimic for HCD cultures which could be used in the mixing time experiments. NaAlg was dissolved in MilliQ water at concentrations between 0.085 and 0.25 g L^{-1} and viscosity was determined at room temperature with the same system and for the same range of shear rates used for the cell viscosity measurements.

2.3. Mixing time determination

Mixing time experiments were performed in the acrylic mimic of the 250 mL bioreactor using the colorimetric acid base reaction technique, known as Dual Indicator System for Mixing Time (DISMT) (Melton et al., 2002). The DISMT method uses two pH indicators: (i) Methyl red, which is red under acidic conditions and (ii) Thymol blue, which is blue under basic condition. Both indicators show yellow in neutral pH ranges of 5.6 – 8.0. For mixing time measurements an acidified DISMT solution was added to the acrylic mimic. Rotational speed was set at the desired speed between 50 and 600 rpm. Fifteen µL of 0.75 M NaOH were added through the liquid addition port and images captured with the iCube camera until a colour change to yellow was observed. For mixing time studies with the recirculation loop, the recirculation pump was initiated simultaneously with agitation. Images taken were analysed and mixing time determined using a purposely written MatLab code (Mathworks, Massachusetts, USA) which measured the change in red, green and blue (RGB) pixels in the images over time. Impeller and baffles were masked to enable accurate analysis of the liquid. Mixing time is defined as a stable value of 95% green pixels meaning the solution colour is yellow with 95% homogeneity at t_M.

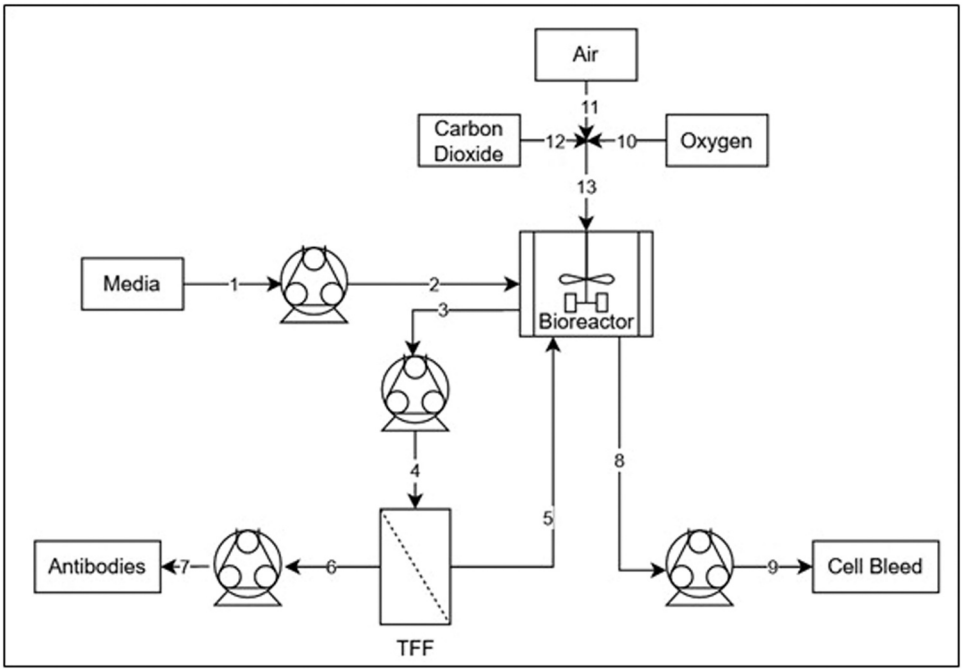

Fig. 2 – Simplified overview of a perfusion bioreactor operation. (1) medium inlet to (2) bioreactor vessel, (3) suspension outlet recirculated using a low shear magnetic levitation pump towards (4) cell retention device - here: membrane based using tangential flow filtration (TFF), (5) cell recirculation loop, (6) supernatant outlet for (7) harvest collection, (8) suspension outlet for (9) cell bleed to maintain stable cell concentrations, (10) oxygen, (11) air, (12) CO_2, (13) gas mixture inlet.

2.4. *Determination of power input and impeller power number*

For the determination of the impeller power number the acrylic mimic of the 250 mL bioreactor was clamped into a chuck jaw on an air bearing and fitted with a dual impeller configuration on an extended impeller shaft. The impeller was connected to a MP-Series Low inertia Servo motor (Rockwell Automation, Milwaukee, USA) and controlled using Ultraware software (Rockwell Automation). The dual impeller configuration was placed at off-bottom impeller clearance of 2.5 cm. The vessel was filled with either water, glycerol or water-glycerol solutions. A force gauge is placed horizontally and the distance from the sensor-jaw contact point to the impeller shaft was measured. Prior to every measurement the force gauge was set to zero, creating a delay time of 30 s. During the delay, the motor was set at rotational speed between 50 and 750 rpm either clockwise (down-pumping) or counter-clockwise (up-pumping). The force gauge measured average force over 45 s after the initial delay.

2.5. *Determination of oxygen mass transfer coefficients*

The k_La measurements were conducted using the dynamic gassing out method, where airflow rates between 25 and 100 mL min^{-1} at agitation speeds between 50 and 600 rpm were investigated. The test liquid was 250 mL CD CHO medium conditioned to room temperature and operational temperature of 37 °C. Dissolved oxygen (DO) levels were measured using an electrolyte DO probe. After saturation is reached, nitrogen sparging is introduced until DO < 5%, subsequently followed by air sparging at the desired gas flow and agitation rates until DO reaches > 50%. The k_La is determined from the slope of the natural log of measured data against time.

2.6. *Cell culture and analytics*

A single GS-CHO K1 cell line producing an IgG monoclonal antibody was used and supplied by Lonza Biologics (Slough, UK). Cells were cultivated in CD CHO medium (Thermo Fisher Scientific Massachusetts, USA) supplemented with 25 µM methyl sulphoximine (MSX). Cultures were placed in a CO_2 incubator (MCO-19AIC, Sanyo) at 37 °C, with 5% CO_2 and were agitated on shaker tables with an orbital diameter of 25 mm (CO_2 Resistant Shaker; Thermo Fisher Scientific). Viable cell concentration as well as viability were measured using a ViCell XR automated viability analyser (Beckman Coulter, California, USA). Samples were diluted with PBS (Gibco, Thermo Fisher Scientific) as required. IgG titres were determined using HPLC (HPLC Agilent 1100 series; Agilent, Santa Clara, USA) with a 1 mL Protein G column (HiTrap Protein G HP; GE Healthcare, Chicago, USA).

2.7. *Perfusion operation*

A bioreactor in perfusion mode was set-up according to the process flow chart shown Fig. 2. DO was set to 30% using a drilled-hole L-sparger, and agitation was initially set to 250 rpm. To maintain the DO agitation was increased stepwise by 30 rpm per day as required to a maximum of 500 rpm. Perfusion was started on day 3, where cell retention was achieved via tangential flow filtration using a hollow fibre mPES TFF with a surface area of 88 cm^2, length of 20 cm and internal diameter of 1 mm (Spektrum® MidiKros; Repligen, Massachusetts, USA). Cell culture was circulated at flowrate of 80 mL min^{-1} using a PuraLev® i30SU pump with sterile, single-use pump head (PuraLev® i30SU; Levitronix, CH). A perfusion rate between 0.5 and 1.8 reactor volumes per day (RV d^{-1}) was applied, where media inlet and supernatant outlet flow rates were controlled using identical peristaltic pumps (101 U/R, Watson-Marlow, Cornwall, UK). Antifoam

Fig. 3 – Photographs of the 250 mL sterilisable bioreactor and acrylic mimic. Both fabricated by the UCL Design and Fabrication Facility. (A) stainless steel 250 mL novel bioreactor for cell culture; (B) acrylic mimic for hydrodynamic studies and engineering characterisation.

was added at 1 mL d^{-1} to control foam levels during the perfusion culture.

3. Results and discussion

The 250 mL bioreactor was specifically designed to meet geometry requirements for perfusion cell cultures and enable cost-effective small-scale process development while maximising the efficiency of the hydrodynamic environment. To this aim, in this section design considerations were discussed and a comprehensive characterisation including gas-liquid mass transfer coefficient, power input and mixing time was presented. Viscosity measurements at working cell densities were examined, leading to the requirement for a non-Newtonian transparent cell mimic to be developed. Mixing time experiments using the newly develop mimic were conducted and implications for impeller spacing and loop recirculation design are presented.

3.1. *Design considerations*

The novel stirred tank geometry bioreactor was designed to enable perfusion operation at small scale. It is common to fabricate lab-scale and benchtop bioreactor from glass, but in this work stainless steel was selected as material for the reactor vessel due to limitations during the fabrication. Stainless steel is biocompatible, sterilisable and gave flexibility to fulfil exact design specifications. In addition, a transparent acrylic mimic was fabricated and utilised for hydrodynamic analysis. Photographic images of both systems are shown in Fig. 3.

A working volume of 250 mL was chosen to remain comparable to other small-scale bioreactors commercially available, including the ambr250® (Sartorius) and the DasBox (Eppendorf). Further, reactor dimensions were selected to maintain a height to diameter ratio between 1 and 1.5, which is typical for cell culture bioreactors (Jossen et al., 2017, Kadic and Heindel, 2011). Although greater aspect ratios facilitate longer residence times within the bioreactor, maximising the potential oxygen transfer and allowing for improved temperature control due to larger surface area to volume ratio, the aspect ratio of 1.1 of the bioreactor presented in this work is within the recommended range. Further, a liquid height equal to 75% of the vessel height is suitable (Ravi, 2017), leaving enough headspace to allow for foaming without overspill and maximising the utilisation of the vessel.

A dual impeller system was selected for this bioreactor, where a down-pumping pitched blade impeller was placed above a Rushton turbine impeller. This was to optimise the reactor performance for HCD perfusion cultures through improved mass transfer, increased k_La and reduced mixing time (Alok, 2014). Literature suggests the implementation of multiple Rushton turbines to achieve optimal gas transfer (Karimi et al., 2013). Previous studies also showed that

Rushton turbine impellers are more efficient in breaking air bubbles, increasing the risk of foaming and cell damage (Karimi et al., 2013, Nienow, 2006, Nienow et al., 2013b). However, these have been shown to induce high shear stress whereas pitched blade impellers are associated with lower shear and are typically used in processes with low mass transfer demand. Very HCD perfusion cultures have an increased demand for O_2 transfer, bubble dispersion and CO_2 stripping (Flickinger, 2010, Karimi et al., 2013). Considering these requirements, the shear sensitivity of the cells and the additive nature of the power number an impeller system consisting of a dual configuration consisting of a down-pumping pitched blade above a Rushton-like turbine impeller was selected. Preliminary studies using different impeller configurations showed that a single Rushton-like impeller does not provide the required mass transfer and a dual impeller configuration resulted in air entrainment from the top and excessive foaming (data not shown).

In addition, baffles of size 0.05 D_T were incorporated to further improve the mass transfer and optimise bioreactor performance for perfusion cultivations. Given the small volume and space restrictions of the system and the large number of probes present during culture, it was decided to incorporate three baffles rather than four. Typically, the bottom of a bioreactor is round-shaped which is preferred for solid suspensions and mixing, as well as to have a reduced dead volume when removing water, cell suspension or medium. However, as the bottom shape does not significantly impact gas-liquid mass transfer, a flat base was chosen for convenience of fabrication. Connectors to a cell retention device were placed in the base, thus facilitating water and medium removal. Given the fact that the 250 mL bioreactor is a non-standard newly designed tank, engineering characteristics must be determined and implemented to support successful scale translation. Particularly engineering characteristics with a significant impact on culture performance, such as k_La, power input per unit volume and mixing time must be evaluated.

3.2. *Oxygen transfer coefficient (k_La)*

Sufficient oxygen supply becomes of concern when operating at HCD and is critical when reproducing performance at different scales. Further, it must be considered that the k_La is dependent on several geometric properties of the vessel and process operation conditions. These include temperature, gas bubble size determined by sparger diameter and mixing characteristics determined by impeller geometry (Middleton, 1992). The gas bubble size was expected to decrease with increasing agitation, thus, an increase of k_La values with increasing agitation was expected. The smaller bubble size provides a larger surface area available for oxygen transfer and longer residence time of the bubbles in the bioreactor. The temperature inversely affects the oxygen solubility. The reducing solubility with increasing temperature would impact the driving force and might facilitate rapid stripping during the gassing out method. In addition to the geometric properties, physical properties of the cell culture such as cell density can influence the magnitude of the k_La values. The utilisation of water or medium for the experimental determination of k_La is not always representative. This is due to consumption, and production of metabolites, as well as consumption of oxygen for cell growth and production of surface-active agents (Garcia-Ochoa and Castro, 2001).

In this work we investigated the oxygen mass transfer and determined the oxygen mass transfer coefficient (k_La) using the dynamic gassing out method. Experiments were performed at room temperature and operating temperature of 37 °C with gas flow rates ranging between 25 and 100 mL min^{-1}. The impeller geometry is fixed across the two temperatures investigated in this work. Agitation rates typical for cell culture processes were chosen for the experimental determination of k_La covering speeds between 50 and 600 rpm. The experimentally obtained k_La values for room temperature and 37 °C are shown in Fig. 4 A and B, respectively. For both temperatures, an increase of k_La values with increasing rotational speed and gas flow rate was observed. At operational conditions (250 rpm, 37 °C, gas flow rate of 50 mL min^{-1}), a k_La of 6 h^{-1} was achieved for the novel 250 mL bioreactor. This lies within the expected range based on previously reported values for mammalian cell culture, which are ranging from 2.5 to 8.5 h^{-1} for a bioreactor at a scale of 250 mL fitted with a pitched blade impeller (Bareither et al., 2013). Schwarz et al. (2020) investigated the impact of different impeller configurations on the mass transfer in a DasBox system retrofitted for perfusion operation. They

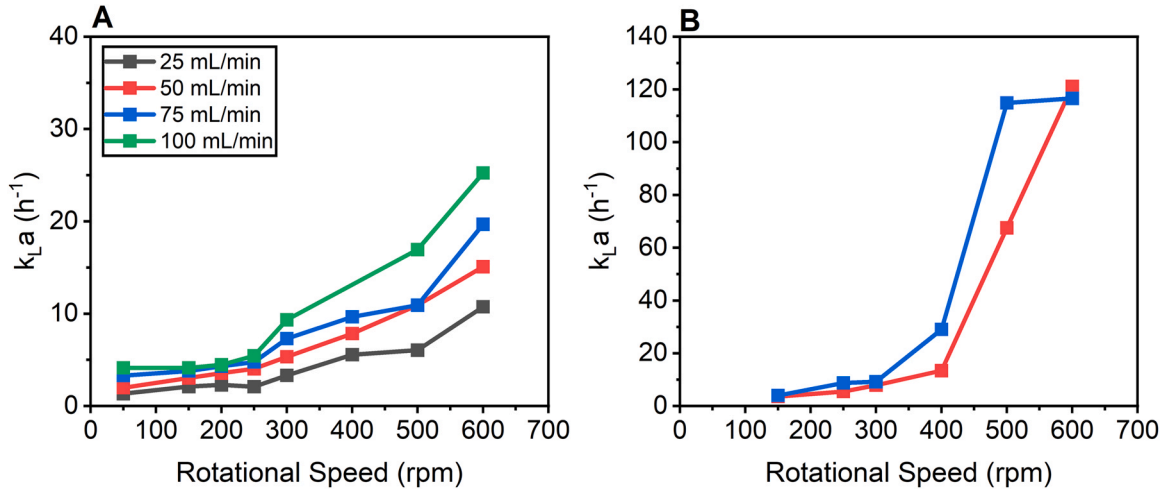

Fig. 4 – Determination of oxygen mass transfer coefficient (k_La) in the 250 mL bioreactor. Measurements were conducted using dynamic gassing out method at gas flow rates of 25–100 mL min^{-1} and N = 100–600 rpm. (A) k_La at room temperature; (B) k_La at 37 °C. Data is represented as average of 2 replicates.

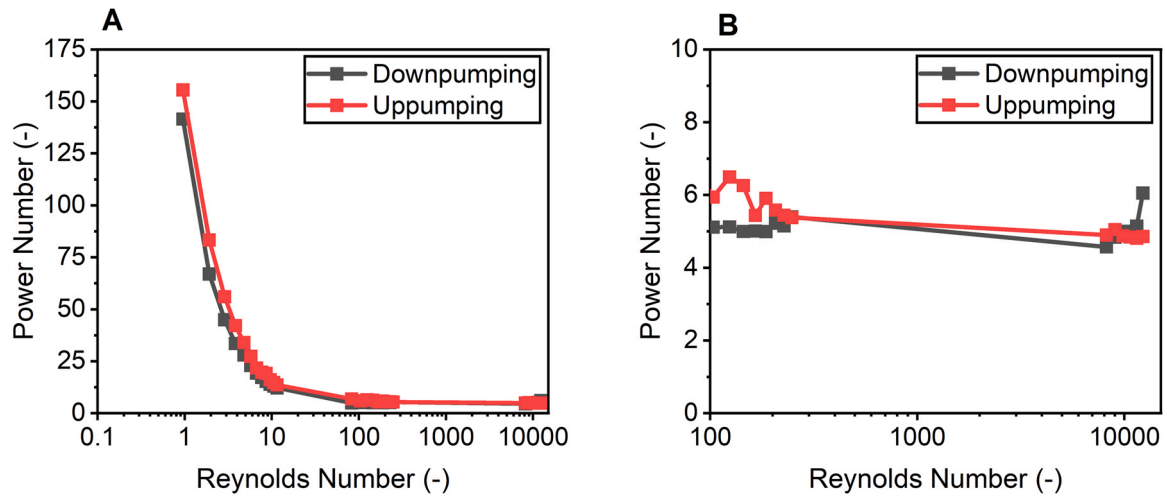

Fig. 5 – Power input measurements; experimentally determined by rotating the 250 mL bioreactor on an air bearing and measuring the applied force at N = 50 – 700 rpm. Vessel was filled with glycerol, water, and water/glycerol mixture to enable adequate measurements at low Reynolds numbers with impellers rotating in down- and up-pumping configurations. (A) power number vs Reynolds Number in down- and up-pumping configurations (B) zoom of A for 100 < Re < 10,000. Data is represented as average of 2 replicates.

reported k_La values of 29.2 h^{-1} and 19.5 h^{-1} with and without additional air sparging, respectively, for a dual impeller system made of a Rushton-like impeller (top) and a pitched blade impeller (bottom), in a reversed order as presented in this work. It is noteworthy that the large differences observed in k_La values could be due to the different vessel geometries and sparger designs. Interestingly, at the operational temperature of 37 °C and above a rotational speed of 400 rpm, the k_La increased drastically whereas at room temperature a similarly drastic increase was not observed (Fig. 4A), thus demonstrating the strong dependence of k_La on temperature and rotational speed. The higher agitation could lead to bubble breakage, which increases surface area and facilitates longer residence times of the gas bubbles in the reactor. Further, in this work CD CHO medium was used as working fluid. As the medium contains salts, sugars and other additives, the liquid phase has different composition at different temperatures, as temperature-sensitive ingredients may degrade. The possible difference in compositions at 37 °C, in comparison to room temperature, could potentially prevent bubble coalescing, hence affecting the k_La, and only becoming apparent at higher agitation rates.

3.3. *Power input*

The power number is a dimensionless number related to the impeller type, impeller blade thickness, and impeller diameter to tank diameter (D_i:D_T) ratio (Chapple et al., 2002). In pitched blade impeller systems, the D_i:D_T is the most significant parameter impacting the power input (Chapple et al., 2002), whereas for Rushton turbine impeller the blade thickness is expected to influence the power input. Reported power numbers for pitched blade impellers vary between 0.25 and 0.75 (Nienow, 2006, Nienow and Miles, 1971) and for Rushton turbines between 4.5 and 6.5. The ratio of impeller blade thickness to impeller diameter is often greater in small scale bioreactors due to fabrication requirements, challenges in fabricating micron-sized blades, in addition to the risk of breakage of very thin blades during operation. In this work this led to the need to accurately determine the power number of the newly designed and non-standard system.

Fig. 5 shows the power number for water, glycerol and a water/glycerol mixture at increasing Reynolds numbers when rotating the impeller in down-pumping and up-pumping modes. Fluids with higher viscosity (glycerol, water/glycerol mixture) than water were required for experiments with rotational speeds sufficiently low that measurements could not be accurately performed with a water-like solution. The viscosity was measured at room temperature at 7.9×10^{-4} and 3.6×10^{-5} m^2 s^{-1} for 100% glycerol and a mixture consisting of 75% glycerol and 25% water, respectively, and these values were used for the Reynolds number calculation. As expected, power numbers were comparable between down-pumping and up-pumping modes for the dual impeller system incorporated in the 250 mL bioreactor given the symmetry of the configuration of the acrylic reactor (Fig. 5). The evaluation of power number against Reynolds number for both configurations showed the expected patterns of decreasing power numbers with increasing Reynolds numbers through the laminar and transitional flow regime as shown in Fig. 5. The impeller power number (N_P) was found to be 4.9 ± 0.2 for the dual impeller system in both up-pumping and down-pumping configurations. This value is within the range of 4.5 – 6.5 for Rushton turbines (Nienow and Miles, 1971). However, accurate power number studies for dual impeller systems are difficult to find in the published literature, and even more so for a dual system using two different impeller types. For all dual systems the power number is largely dependent on the impeller spacing (Bates et al., 1963) as well as on the blade thickness to impeller diameter ratio (Chapple et al., 2002), among other factors. Bates et al. (1963) measured power characteristics for dual impeller systems and found that, for a mixed RT-PBT configuration, the total power number was equal to the sum of impeller power numbers when impeller spacing was equal to one impeller diameter, which is the distance selected in this work. Chapple et al. (2002) compared their power number results and those of others for a RT at different blade thicknesses to impeller diameter ratios and found that a Rushton turbine had a power number of approx. 4 for an impeller thickness to impeller diameter ratio equal to 0.05 as in this work. Given that power numbers for pitched blade

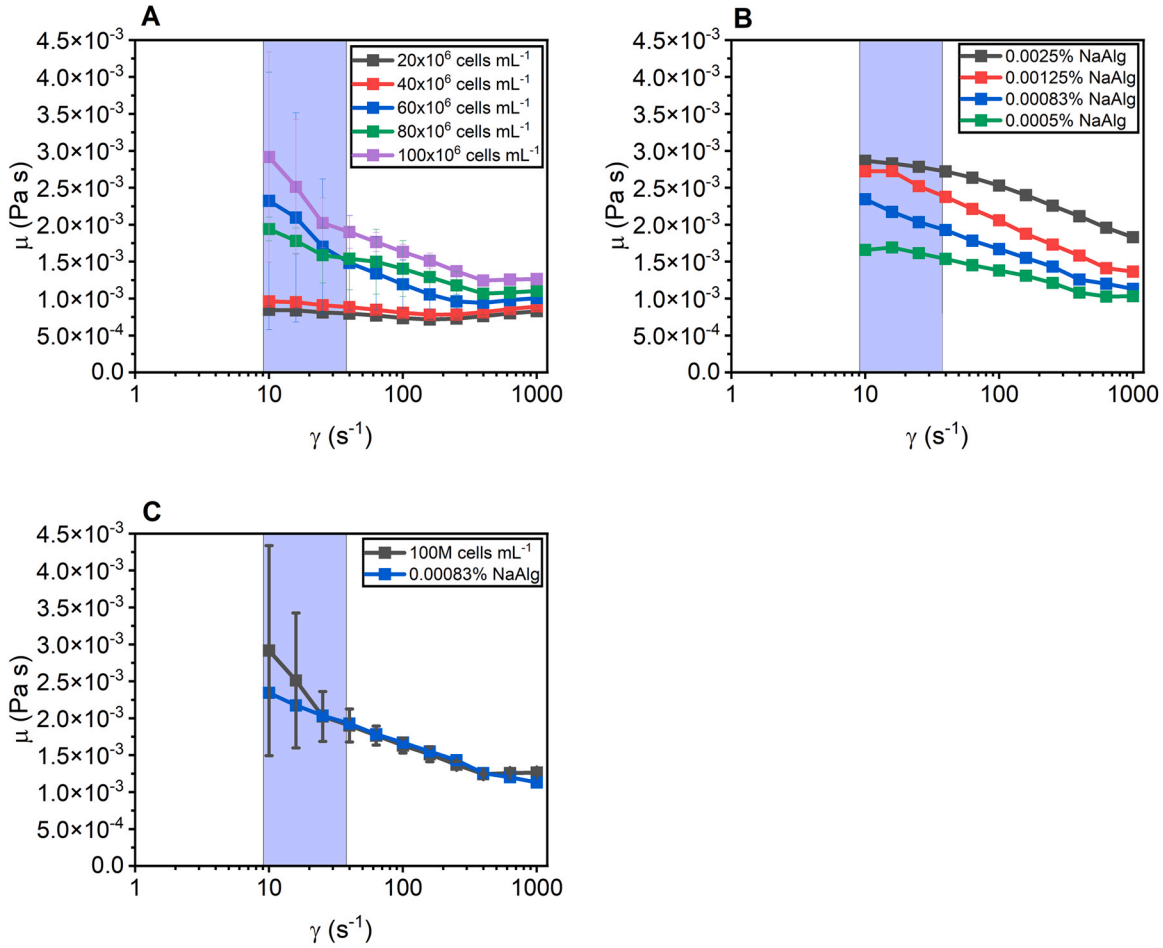

Fig. 6 – Viscosity measurements of CHO cell culture at densities of 20 – 100 × 10^6 cells mL^{-1} and development of model fluid to mimic CHO cell suspension of 100×10^6 cells mL^{-1}. (A) viscosity (μ) vs shear rate (γ); (B) μ vs γ NaAlg solutions; (C) viscosity comparison of CHO cell suspensions at 100×10^6 cells mL^{-1} and 0.0083% NaAlg solution. Blue shaded region represents $\gamma < 40\ s^{-1}$ where measurements are subject to a high degree of variability. Average values and standard deviation calculated using N = 3 replicates.

turbines are reported to be between 0.5 and 1.2, depending on geometrical characteristics, a total power number of 4.9 for the dual impeller system used in this work is justified. CFD simulations are ongoing to further investigate the power consumption, the resulting flow and level of impeller interaction for the selected design. It was expected to observe similar power numbers for the down- and up-pumping configurations as the acrylic mimic had no probes and was thus symmetrical during these measurements. It should be noted that the power number might change in the presence of probes and this is the subject of further investigations.

3.4. *Viscosity in HCD cell cultures and impact of HCD on mixing dynamics*

When operating a perfusion process at HCD, it is important to consider possible changes in the rheological properties of the liquid occurring throughout the process. While suspensions during fed-batch operations have rheological properties similar to water, this is expected to be different for very HCD cultivations. In particular the viscosity is expected to change, however measurements of rheological properties of representative cell culture suspension at increasing viable cell concentration (VCC) are rarely conducted and such data are currently not available in the published literature.

To mimic mixing time experimentations of HCD cultures, the viscosity of HCD CHO cell cultures was measured at different cell concentrations (20–100 ×10^6 cells mL^{-1}) and at constant temperature (T = 37 °C). Fig. 6 presents viscosity measurements of CHO cell culture at different cell concentrations and the development of a model fluid to mimic HCD cell culture. Fig. 6A shows that at VCCs below 40 × 10^6 cells mL^{-1} mixtures showed similar rheological properties as water at 0.8 – 1.0 × 10^{-3} Pa s for $\gamma = 10 - 1000\ s^{-1}$. However, suspensions at higher VCCs exhibit a non-Newtonian shear-thinning behaviour, where viscosity decreases with increasing shear rate, and minimum apparent viscosity values of 0.98, 1.0, and 1.3 × 10^{-3} for 60, 80 and 100 × 10^6 cells mL^{-1} were obtained, respectively, at a shear rate of 1000 s^{-1}. Further, viscosities increase up to 3-fold at HCD compared to conventional cell density (CCD) at $\gamma < 40\ s^{-1}$ (Fig. 6A). For shear rates below 40 s^{-1}, high variability of viscosity is observed over all VCCs due to the shear rate lying outside the range of accuracy for the rheometer used.

A typical perfusion bioreactor run aims to achieve a stable cell concentration of 100×10^6 cells mL^{-1}, the viscosity and fluid type determined for this cell concentration was utilised for calculations relating to HCD operation in this bioreactor. The average shear rate at which measurements were conducted was 45.4 s^{-1} relating to an apparent viscosity of 1.8 × 10^{-3} Pa s. HCD cell suspensions at operating conditions

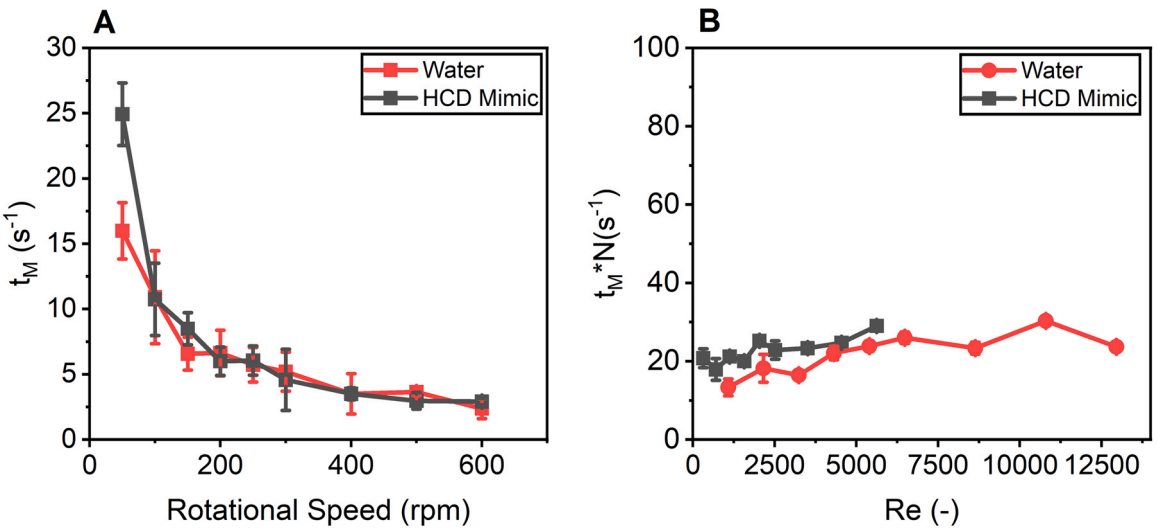

Fig. 7 – Influence of viscosity at HCD on mixing dynamics. H_i = 2 cm. (A) mixing time vs rotational speed; (B) t_M*N vs Reynolds Number. For N < 150 rpm, data represents 8 replicates, for N = 150–300 rpm data represents 5 replicates and for N > 300 rpm data represents 3 replicates with standard deviation, respectively.

had a viscosity approximately twice that of water. However, this meant that mixing time experiments, usually conducted using water-like viscosity solutions, might not accurately represent HCD cultures. Hence, to ensure accurate representation of HCD viscosity in a transparent model fluid required for mixing time experimentation, solutions of sodium alginate at different concentrations (NaAlg, 5×10^{-4} – 2.5×10^{-3}% v/v) were made and their apparent viscosity measured at different shear rates. Results are shown in Figs. 6 B and C. Good similarity was observed between the viscosity results of the solution at 8.3×10^{-4}% v/v NaAlg concentration to CHO cell suspensions with a VCC of 100×10^{6} cells mL^{-1} at $\gamma > 37\,s^{-1}$ (Fig. 6C). Mixing time experiments were then conducted using the NaAlg solution at 8.3×10^{-4}% to enable prediction of mixing hydrodynamics at HCD and results are presented in Fig. 7A. The CHO cell cultures at high cell concentration and thus the HCD mimic have shear thinning properties at increasing agitation ranging from 2.4×10^{-3} Pa s at 50 rpm to 1.6×10^{-3} Pa s at 600 rpm. Figs. 7A and 7B shows mixing time results obtained at increasing rotational speed and increasing Reynolds number for both solutions. The HCD mimic showed a nearly 2-fold increased mixing time compared to water at the lowest rotational speed investigated in this work (Fig. 7A). The dimensionless mixing time against Reynolds showed similarities between water and the HCD mimic with values between 13 - 24 for water and 18 – 29 for the HCD mimic, respectively, at Re < 5600 (Fig. 7B). It was expected to obtain lower mixing numbers for the dual impeller configuration than for single impeller configurations previously presented in literature. For a single Rushton-like impeller mixing numbers of 24 (Liepe et al., 1998) and for single pitched blade impeller mixing numbers in range of 30 – 34 (Liepe et al., 1998, Kaiser et al., 2011) were reported. A constant mixing number was obtained across the Reynolds number range investigated. This means that fluid flow is likely to be fully turbulent well below values commonly defined as boundary between transition and turbulent (Re = 10,000). Similar results were previously reported in literature, where turbulent fluid flow was achieved for Reynolds numbers as low as 5600 (Samaras et al., 2020a, Zhang et al., 2017). It is noted that the non-Newtonian behaviour of the CHO cell lines at high cell concentrations is mild, and the viscosity does not increase significantly above that of water, hence for the cell concentrations studied in this work a water-like solution is a sufficient model of fluid. It is very critical that the type of fluid and the change in viscosity during the process are considered and accurately quantified, for example for different concentrations, mammalian cell lines and media combinations, to ensure Reynolds number calculations and equipment design considerations are made using the correct viscosity values.

3.5. *Impact of H_i on mixing time*

In addition to the measurement of power number and k_La, mixing time (t_M) can be used as scaling parameter and is often determined to quantify mixing efficiency. In this work, the mixing time was measured at varying impeller locations to ensure the design which provided the best mixing was selected. In addition, flat bottom vessels are prone to dead zones (Samaras et al., 2020b), hence, to achieve homogeneity of the bulk liquid, two impeller off-bottom clearances were evaluated for the dual impeller system, namely a clearance of 0.25:1 H_i:H_T (H_i = 2.5 cm) and a clearance of 0.1:1 H_i:H_T (H_i = 1 cm), and mixing experiments were conducted at both configurations.

Fig. 8 shows mixing time measurements obtained using water as working fluid at different rotational speeds and at increasing Reynolds number. For N < 150 rpm (Re < 2600) a difference in mixing performance between the two configurations can be observed, where faster mixing times were observed when the impeller was set at the higher clearance. At N > 150 rpm, mixing times observed were comparable between both configurations, tending asymptotically to values of 3 – 6 s^{-1} as shown in Fig. 8A. The evaluation of the dimensionless mixing number t_M *N and its variation with Reynolds number is presented in Fig. 8B, showing comparable results for both configurations. Further, an increase of t_M *N was observed throughout the transitional flow regime. This is most likely due to the fact that the technique has a lower measurement limit and mixing time is approaching values close to or outside the range of measurement. Overall, for the off-bottom clearance with a H_i = 2.5 cm the

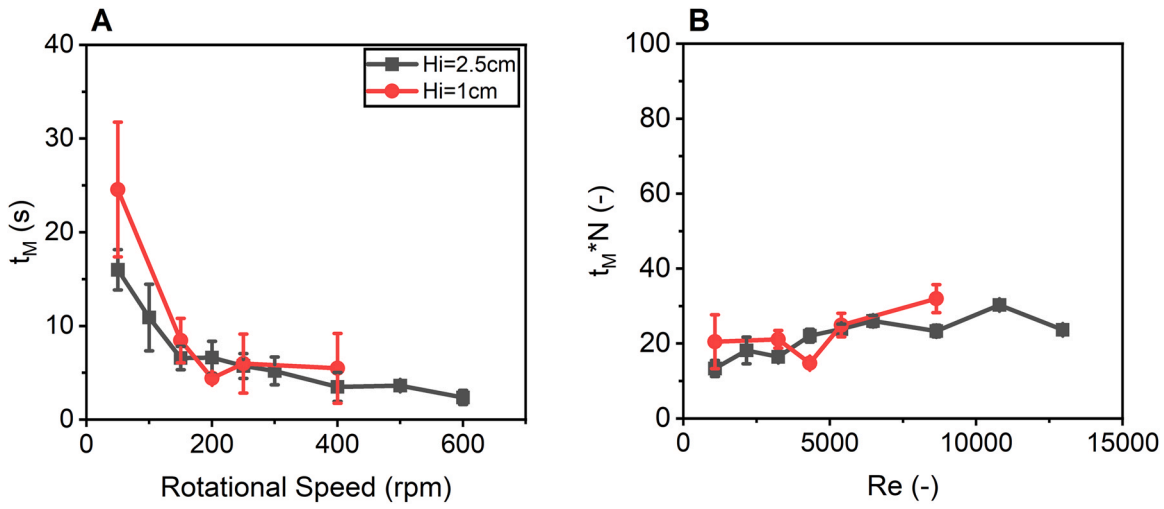

Fig. 8 – Mixing time evaluation in 250 mL bioreactor fitted with dual pitched-blade and Rushton-type impeller at H_i = 1 and 2.5 cm using DISMT method. (A) mixing time at N = 50–600 rpm for H_i = 1 and 2.5 cm (B) t_M*N vs Reynolds Number for H_i = 1 and 2.5 cm. For N < 150 rpm, data represents 8 replicates, for N = 150–300 rpm data represents 5 replicates and for N > 300 rpm data represents 3 replicates with standard deviation, respectively.

dimensionless mixing number values, t_M *N, were more consistent and found to be in the range of 14 – 26 compared to 14 – 34 for H_i = 1 cm. Comparisons of these results with previously published data are challenging as mixing numbers have been often reported only for one impeller systems. As an example, for the Rushton-like impeller mixing number values of 24 were reported (Liepe et al., 1998), while for pitched blade impellers mixing numbers of 30 – 34 were obtained (Liepe et al., 1998, Kaiser et al., 2011). The mixing dynamics in a dual impeller system would likely depend not only on each impeller geometry but also on the spacing between the two and interactions with other internals and it is difficult to predict how the mixing number would vary in these cases if not directly measured.

3.6. *Impact of recirculation loop*

While fed-batch processes are characterised by feed addition, bioreactors in perfusion mode are similar to a chemostat as they are characterised by a continuous medium removal compensated by feed addition. However, differently from a chemostat, a perfusion bioreactor has an additional cell retention and recirculation loop to return cells back to the bioreactor. Cell suspension is continuously circled through a cell retention device, separating spent medium and product from cells. The cells are then returned to the bioreactor, whereas the supernatant is transferred to harvest tanks (Bielser et al., 2018). In large scale systems the cell recirculation is often designed to be below the liquid level (Martens et al., 2014). In small-scale systems, the return of cells is often from above the liquid level and delivered from the headplate, due to space limitations inside the bioreactor. In this work the impact of the recirculation loop on the bulk hydrodynamics was investigated for two configurations, namely a recirculation from the headplate (above the liquid level) and from a side port (below the liquid level). Mixing time was measured at increasing rotational speeds for both configurations and compared to mixing times without recirculation using water as model fluid and results are presented in Fig. 9 A and B. The recirculation flow rate was held constant at 80 mL min^{-1}, which is equal to the operational flow rate used in the biological experiments. Overall, the mixing times in the bioreactor with recirculation below the liquid level were comparable to those obtained without recirculation, and this was noted across the range of agitation speeds tested (Fig. 9A). Mixing times of 22 ± 4.4 s^{-1} for the bioreactor with side recirculation and 23 ± 2.4 s^{-1} with no recirculation were obtained at a rotational speed of 50 rpm. In contrast, the mixing time with top recirculation at the same speed was significantly lower and equal to 12 ± 1.9 s^{-1}. The increment seen for the side port recirculation resulted from the return of fluid below the liquid level, whereas for the top recirculation the returned cell suspension was added above the liquid level. The latter induced a different mixing pattern and possibly higher turbulence levels, resulting in lower mixing times when top recirculation was used at the same rotational speed. At agitation speeds higher than 200 rpm, mixing times become comparable for all configurations tested and for agitation speeds greater than 250 rpm, mixing times of 6.0 ± 1.1 s^{-1}, 3.8 ± 0.5 s^{-1}, and 4.1 ± 0.7 s^{-1} were obtained for the bioreactor with no, side, and top recirculation, respectively. Detailed CFD simulations are ongoing to better understand the impact of the recirculation location and provide insight on the reasons behind the observed results.

Fig. 9B shows the dimensionless mixing number variation at increasing Reynolds number with no, side and top port recirculation configuration. The presence of the recirculation does not have a significant impact on the flow regime inside the bioreactor. At Re > 2000, t_M *N is consistent for top and side port configurations, however, for Re < 2000, a decrease of t_M *N was observed for vessels with top recirculation configurations (Fig. 9B). This was most likely due to increased turbulence within the bioreactor induced from the cell return above the liquid level. In contrast, the absence of the recirculation loop resulted in higher t_M *N values across the range of Reynolds numbers. This suggests that recirculation affects the hydrodynamics of the bioreactor system at agitation speed within the range used for biological experiments in this bioreactor.

Examining the influence of the perfusion recirculation on mixing dynamics at operational recirculation flow rate

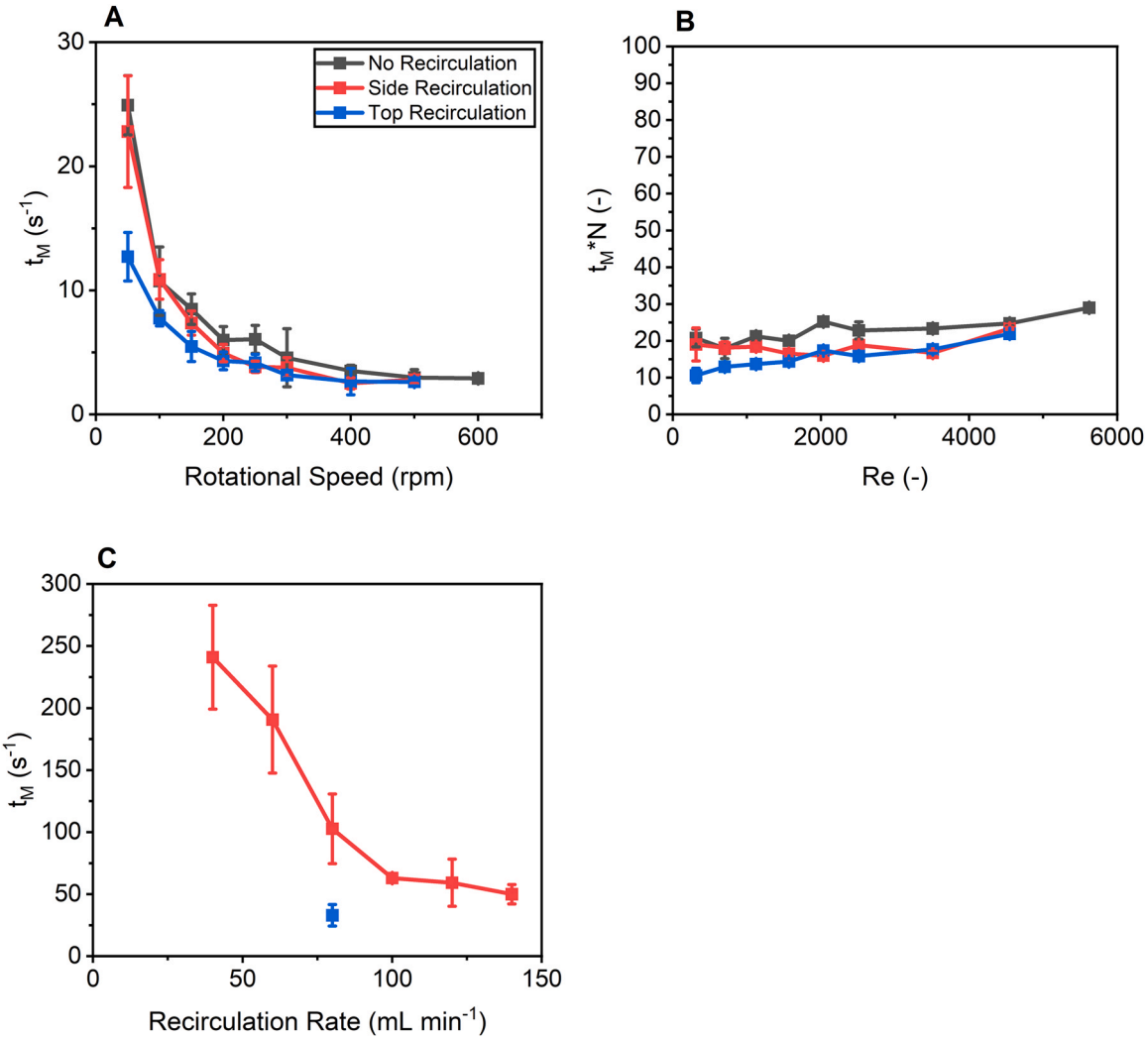

Fig. 9 – Influence of perfusion recirculation on mixing dynamics with return from side or top port and at a recirculation flow rate of 80 mL min^{-1}. N = 50 – 600 rpm, H_i = 2 cm, mixed with DISMT HCD mimic solution. (A) mixing time vs rotational speed; (B) t_M*N vs Reynolds Number. For N < 150 rpm, data represents 8 replicates, for N = 150–300 rpm data represents 5 replicates and for N > 300 rpm data represents 3 replicates with standard deviation, respectively. (C) mixing time vs recirculation rate, recirculation from side port (40 – 140 mL min^{-1}) and from top port at 80 mL min^{-1}, N = 0 rpm. Data represents 3 replicates with standard deviation.

showed that for rotational speeds typical for cell culture processes (> 250 rpm) comparable mixing dynamics were obtained for side and top recirculation. In order to better understand the impact of the recirculation loop, mixing time experiments were conducted for a range of recirculation flowrates through the side port without additional agitation, and results are presented in Fig. 9C. Flowrates ranging from 40 to 140 mL min^{-1} were investigated for the side port configuration, while the flow rate for the top port configuration remained constant at the operational flowrate of 80 mL min^{-1}. The increase of the recirculation flowrate resulted in a reduction of mixing time for the side port experiments. Mixing times of 240 ± 41 s^{-1} and 50 ± 7 s^{-1} at 40 mL min^{-1} and 140 mL min^{-1}, respectively, were obtained. Comparing both configurations at the operational flowrate of 80 mL min^{-1}, it is noted that recirculating from the top port resulted in lower mixing times of 32 ± 8 s^{-1} compared to 102 ± 28 s^{-1} for side port recirculation (Fig. 9C). The lower mixing times obtained for the top port in comparison to the side port recirculation in non-agitated systems is an indication of higher turbulence levels likely present for top fluid additions. While the difference between mixing times was significant in the absence of agitation, the impact was less significant when agitation was introduced.

Based on these findings the side port recirculation was utilised in the design of the 250 mL perfusion bioreactor due to space restrictions on the headplate and to limit the turbulence experiences by the cells during cultivation. The possible reduction of turbulence levels at the top of the reactor was beneficial for the cell culture as it reduced foaming, a common problem in high cell density processes, which in turn reduced cell damage via bubble bursting effect. This solution would also limit the use of anti-foaming agents, known to affect cellular health through osmolality.

3.7. *Development of perfusion methodology in the 250 mL bioreactor*

Following the design and characterisation of the bioreactor, perfusion cell culture experiments at varying perfusion rates were carried out to show the capabilities of the system and validate the bioreactor for this specific operation. The system was operated at perfusion rates of 0.5, 1.0 and 1.8 RV d^{-1} and cell retention was achieved via a TFF system with a

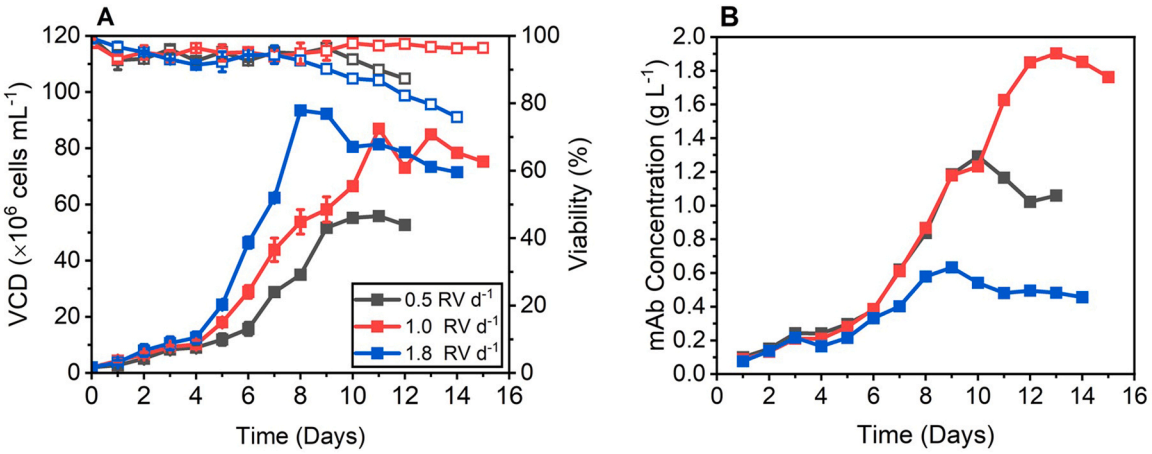

Fig. 10 – CHO cell culture in a 250 mL perfusion bioreactor at different perfusion rates. Cells were seeded at 2 × 106 cells mL^{-1} and cultures in CD CHO medium blended with 15% Feed B (v/v). Perfusion was started on day 3 at a perfusion rate of 0.5, 1 and 1.8 RV d^{-1}. Cell retention was achieved with a TFF and a recirculation flow rate of 80 mL min^{-1}. (A) VCC (filled) and viability (open) (B) mAb concentration. Mean of N = 2 replicates. Error bars indicate standard deviation.

recirculation flow rate of 80 mL min^{-1}. Fig. 10 A and B show, perfusion cultures were successfully conducted for all three perfusion rates, however significant differences regarding cell growth and productivities were observed. Cultures with an exchange rate of 0.5 RV d^{-1} achieved maximum VCCs of 55×10^6 cells mL^{-1} on day 11 and maintained high viabilities (> 88%) for the duration of the culture. Cultures with the highest exchange rate of 1.8 RV d^{-1} achieved significantly higher VCC peaking at 96×10^6 cells mL^{-1} on day 8 but observed a reduction of viability to 75% from day 8. In comparison, cultures perfused at the intermediate perfusion rate of 1 RV d^{-1} achieved VCCs up to 86×10^6 cells mL^{-1} which were maintained over the duration of several days with viabilities > 96% (Fig. 10A).

Monoclonal antibody titres were highest in cultures with perfusion rate of 1.0 RV d^{-1}, obtaining a maximum titre of 1.9 g L^{-1} (Fig. 10B). At the highest perfusion rate of 1.8 RV d^{-1} the product stream was diluted, thus resulting in lower maximum titres of 0.6 g L^{-1} whereas for the lowest perfusion rate of 0.5 RV d^{-1} the product was concentrated resulting in higher titres, reaching a maximum value of 1.3 g L^{-1}. However, despite the lower titres obtained at the highest perfusion rate, the volumetric productivity was improved compared to cultures with low perfusion rates, with productivity values of 0.64 and 0.32 g L^{-1} d^{-1} for 1.8 and 0.5 RV d^{-1}, respectively. Highest volumetric productivities of 0.87 g L^{-1} d^{-1}were obtained in culture with a perfusion rate of 1 RV d^{-1}. This was due to the improvements in the maximum titres, which outweigh the decrease of product volume. Further, cell specific productivities (q_{mAb}) were comparable over all perfusion rates achieving values of 23.7, 22.1, and 23.6 pg cell^{-1} d^{-1} for perfusion rates of 0.5, 1.0, and 1.8 RV d^{-1}, respectively.

Perfusion cultures were successfully implemented in the 250 mL bioreactor for a range of perfusion rates. The L-sparger in combination with the dual impeller system provided adequate k_La values to enable HCD, where agitation was started at 250 rpm and increased stepwise to a maximum of 310 rpm on day 8. The TFF system was able to retain cells throughout the cultivation duration maintaining a separation efficiency of 100%. Pressure build ups as indicators for membrane pore clogging were not observed. Changes in perfusion rate were managed by varying the inlet and outlet flowrate through adaptation of the pump rate of the peristaltic pumps. The minimum feasible perfusion rate was 0.5 RV d^{-1}. Lower perfusion rates could not be implemented as the impact of flowrate fluctuations (± 0.02 mL min^{-1}) become hindering over time and was greatest at low perfusion rates. Maximum VCC of 93×10^6 cells mL^{-1} were achieved for cultures perfused at 1.8 RV d^{-1}. However, at this flowrate significant foaming was observed, likely impacting cell viability due to bubble bursting (Walls et al., 2017) and indirectly by higher osmolality values due to antifoam addition. Cultures with a perfusion rate of 1.0 RV d^{-1} generated improved titres and volumetric productivities despite lower VCCs in comparison to other perfusion rates tested. Performance at this perfusion rate was found to be comparable to perfusion cultures conducted in DasBox bioreactors at identical scale, where cell densities of 100×10^6 cells mL^{-1} for a GS-CHO cell line were reported (Chotteau, 2017). Moreover, it is noteworthy that the 250 mL bioreactor was capable of supporting HCD cultures close to typical cell densities of 100×10^6 cells mL^{-1} commonly reported for perfusion cell culture (Chotteau, 2015, Clincke et al., 2013b).

4. Conclusion

This paper presented the design and characterisation of a sub-litre bioreactor to be used for cell culture operations in perfusion mode. The 250 mL bioreactor was designed to maximise the efficiency of the hydrodynamic environment and mass transfer, in addition to other geometry and space constraints. During bioprocess development, the engineering characterisation is important to gain a deep understanding of the hydrodynamics within the system to inform successful scaling efforts. Values for k_La, power input and mixing time achieved with the novel 250 mL bioreactor were within the ranges given in literature for larger scale bioreactors. Furthermore, the design of a multiple impeller system improved oxygen mass transfer and allowed successful perfusion operation at industrially relevant cell densities. Further, recent improvements around fabrication of small sterilisable impellers could make additional studies for different impeller configurations possible. In the future a combined experimental and simulation flow analysis could provide more insights and further extend the

characterisation data set for this bioreactor. Several perfusion cell cultures were successfully performed at different perfusion rates in the novel bioreactor, achieving maximum VCCs similar to targeted large scale industry operations. The results presented shows the applicability of the system as a tool for bioprocess development to ensure cost and time efficiency in early-stage development studies. Most importantly, the bioreactor design and characterisation results were fully disclosed with the intention to enable replication in other academic laboratories, including the option of further tailoring to a specific use, with the view this would help to further adopt the perfusion technology in academia, and furthering research in the area of biopharmaceutical manufacturing.

Funding

Marie Dorn's studentship was co-funded by the AZ-UCL Centre of Excellence and Engineering and Physical Sciences Research Council (EPSRC), the Centre for Doctoral Training [Grant ref: EP/S021868/1]. Molly Tregidgo's studentship was supported by the UK Engineering and Physical Sciences Research Council (EPSRC) Centre for Doctoral Training in Bioprocess Engineering Leadership [Grant ref: EP/L01520X/1].

Declaration of Competing Interest

The authors declare that they have no known competing financial interests or personal relationships that could have appeared to influence the work reported in this paper.

Acknowledgements

The authors would like to acknowledge the support and supervision of Astrazeneca and the AZ-UCL Centre of Excellence (CoE) for their constructive discussions and insight. We would like to thank Mark Brower and Nuno Pinto at Merck & Co Inc. for scientific support and Merck & Co Inc. for financial support of the EngD studentship.

References

Alok, S., 2014. Effect of different impellers and baffles on aerobic stirred tank fermenter using computational fluid dynamics. J. Bioprocess. Biotech. 04.

Arnold, L., Lee, K., Rucker-Pezzini, J., Lee, J.H., 2019. Implementation of fully integrated continuous antibody processing: effects on productivity and COGm. Biotechnol. J. 14, e1800061.

Bareither, R., Bargh, N., Oakeshott, R., Watts, K., Pollard, D., 2013. Automated disposable small scale reactor for high throughput bioprocess development: a proof of concept study. Biotechnol. Bioeng. 110, 3126–3138.

Bates, R.L., Fondy, P.L., Corpstein, R.R., 1963. Examination of some geometric parameters of impeller power. Ind. Eng. Chem. Process Des. Dev. 2, 310–314.

Betts, J.I., Baganz, F., 2006. Miniature bioreactors: current practices and future opportunities. Micro Cell Fact. 5, 21.

Bielser, J.M., Wolf, M., Souquet, J., Broly, H., Morbidelli, M., 2018. Perfusion mammalian cell culture for recombinant protein manufacturing - a critical review. Biotechnol. Adv. 36, 1328–1340.

Chapple, D., Kresta, S.M., Wall, A., Afacan, A., 2002. The effect of impeller and tank geometry on power number for a pitched blade turbine. Chem. Eng. Res. Des. 80, 364–372.

Chotteau, V., 2015. Perfusion processes. In: Al-rubeai, M. (Ed.), Animal Cell Culture. Springer, Cham.

Chotteau, V. Process development in screening scale bioreactors and perspectives for very high cell density perfusion. In: FARID, S., GOUDAR, C., ALVES, P. & WARIKOO, V., eds. Integrated Continuous Biomanufacturing III, 2017. ECI Symposium Series.

Clincke, M.F., Molleryd, C., Samani, P.K., Lindskog, E., Faldt, E., Walsh, K., Chotteau, V., 2013a. Very high density of Chinese hamster ovary cells in perfusion by alternating tangential flow or tangential flow filtration in WAVE Bioreactor-part II: applications for antibody production and cryopreservation. Biotechnol. Prog. 29, 768–777.

Clincke, M.F., Molleryd, C., Zhang, Y., Lindskog, E., Walsh, K., Chotteau, V., 2013b. Very high density of CHO cells in perfusion by ATF or TFF in WAVE bioreactor. Part I. Effect of the cell density on the process. Biotechnol. Prog. 29, 754–767.

Croughan, M.S., Konstantinov, K.B., Cooney, C., 2015. The future of industrial bioprocessing: batch or continuous? Biotechnol. Bioeng. 112, 648–651.

Farid, S.S., 2019. Integrated continuous biomanufacturing: industrialization on the horizon. Biotechnol. J. 14, e1800722.

Flickinger, M.C. 2010. Encyclopedia of industrial biotechnology: bioprocess, bioseparation, and cell technology / edited by Michael C. Flickinger, Oxford, Wiley-Blackwell.

Gagliardi, T.M., Chelikani, R., Yang, Y., Tuozzolo, G., Yuan, H., 2019. Development of a novel, high-throughput screening tool for efficient perfusion-based cell culture process development. Biotechnol. Prog. 35, e2811.

Garcia-Ochoa, F., Castro, E.G., 2001. Estimation of oxygen mass transfer coefficient in stirred tank reactors using artificial neural networks. Enzym. Micro Technol. 28, 560–569.

Hsu, W.T., Aulakh, R.P., Traul, D.L., Yuk, I.H., 2012. Advanced microscale bioreactor system: a representative scale-down model for bench-top bioreactors. Cytotechnology 64, 667–678.

Janoschek, S., Schulze, M., Zijlstra, G., Greller, G., Matuszczyk, J., 2019. A protocol to transfer a fed-batch platform process into semi-perfusion mode: The benefit of automated small-scale bioreactors compared to shake flasks as scale-down model. Biotechnol. Prog. 35, e2757.

Jin, L., Wang, Z.S., Cao, Y., Sun, R.Q., Zhou, H., Cao, R.Y., 2021. Establishment and optimization of a high-throughput mimic perfusion model in ambr((R)) 15. Biotechnol. Lett. 43, 423–433.

Jossen, V., Eibl, R., Portner, R., Kraume, M., Eibl, D., 2017. Stirred bioreactors: current state and developments, with special emphasis on biopharmaceutical production processes. Curr. Dev. Biotechnol. Bioeng.: Bioprocess., Bioreact. Controls 179–215.

Kadic, E. & Heindel, T.J. 2011. Hydrodynamic Considerations in Bioreactor Selection and Design. American Society of Mechanical Engineers, Fluids Engineering Division (Publication) FEDSM, 1, 2149–2159.

Kaiser, S.C., Eibl, R., Eibl, D., 2011. Engineering characteristics of a single-use stirred bioreactor at bench-scale: The Mobius CellReady 3L bioreactor as a case study. Eng. Life Sci. 11, 359–368.

Karimi, A., Golbabaei, F., Mehrnia, M.R., Neghab, M., Mohammad, K., Nikpey, A., Pourmand, M.R., 2013. Oxygen mass transfer in a stirred tank bioreactor using different impeller configurations for environmental purposes. Iran. J. Environ. Health Sci. Eng. 10, 6.

Kesik-Brodacka, M., 2018. Progress in biopharmaceutical development. Biotechnol. Appl. Biochem 65, 306–322.

Konstantinov, K.B., Cooney, C.L., 2015. White paper on continuous bioprocessing May 20-21, 2014 continuous manufacturing symposium. J. Pharm. Sci. 104, 813–820.

Liepe, F., Sperling, R. & Jembere, S. 1998. Rührwerke: theoretische Grundlagen, Auslegung und Bewertung, Fachhochsch.

Mahal, H., Branton, H., Farid, S.S., 2021. End-to-end continuous bioprocessing: impact on facility design, cost of goods, and cost of development for monoclonal antibodies. Biotechnol. Bioeng. 118, 3468–3485.

Martens, D.E., Van Den End, E.J., Streefland, M., 2014. Configuration of bioreactors. Methods Mol. Biol. 1104, 285–311.

Melton, L.A., Lipp, C.W., Spradling, R.W., Paulson, K.A., 2002. DISMT - determination of mixing time through color changes. Chem. Eng. Commun. 189, 322–338.
Middleton, J.C., 1992. Gas–liquid dispersion and mixing. In: Edwards, M.F., Harnby, N., Nienow, A.W. (Eds.), Mixing in the Process Industries, 2 ed..,. Elsevier.
Narayanan, H., Sponchioni, M., Morbidelli, M., 2022. Integration and digitalization in the manufacturing of therapeutic proteins. Chem. Eng. Sci. 248 117159-117159.
Nienow, A.W., 1997. On impeller circulation and mixing effectiveness in the turbulent flow regime. Chem. Eng. Sci. 52, 2557–2565.
Nienow, A.W., 2006. Reactor engineering in large scale animal cell culture. Cytotechnology 50, 9–33.
Nienow, A.W., Miles, D., 1971. Impeller power numbers in closed vessels. Ind. Eng. Chem. Process Des. Dev. 10 41-&.
Nienow, A.W., Langheinrich, C., Stevenson, N.C., Emery, A.N., Clayton, T.M., Slater, N.K., 1996. Homogenisation and oxygen transfer rates in large agitated and sparged animal cell bioreactors: Some implications for growth and production. Cytotechnology 22, 87–94.
Nienow, A.W., Rielly, C.D., Brosnan, K., Bargh, N., Lee, K., Coopman, K., Hewitt, C.J., 2013a. The physical characterisation of a microscale parallel bioreactor platform with an industrial CHO cell line expressing an IgG4. Biochem. Eng. J. 76, 25–36.
Nienow, A.W., Scott, W.H., Hewitt, C.J., Thomas, C.R., Lewis, G., Amanullah, A., Kiss, R., Meier, S.J., 2013b. Scale-down studies for assessing the impact of different stress parameters on growth and product quality during animal cell culture. Chem. Eng. Res. Des. 91, 2265–2274.
Rathore, A.S., Winkle, H., 2009. Quality by design for biopharmaceuticals. Nat. Biotechnol. 27, 26–34.
Ravi, R., 2017. Reactor design—general principles (ed). Coulson and Richardson's Chemical Engineering, fourth ed. Elsevier.
Samaras, J.J., Ducci, A., Micheletti, M., 2020a. Flow, suspension and mixing dynamics in DASGIP bioreactors, part 2. AIChE J. 66.
Samaras, J.J., Micheletti, M., Ducci, A., 2020b. Flow, suspension, and mixing dynamics in DASGIP bioreactors: part 1. AIChE J. 66.
Satorius. 2021. Ambr250 High throughput Perfusion [Online]. Available: https://www.sartorius.com/en/products/fermentation-bioreactors/ambr-multi-parallel-bioreactors/ambr-250-high-throughput-perfusion [Accessed 10/02/2023 2023].
Schwarz, H., Zhang, Y., Zhan, C., Malm, M., Field, R., Turner, R., Sellick, C., Varley, P., Rockberg, J., Chotteau, V., 2020. Small-scale bioreactor supports high density HEK293 cell perfusion culture for the production of recombinant Erythropoietin. J. Biotechnol. 309, 44–52.
Sewell, D.J., Turner, R., Field, R., Holmes, W., Pradhan, R., Spencer, C., Oliver, S.G., Slater, N.K., Dikicioglu, D., 2019. Enhancing the functionality of a microscale bioreactor system as an industrial process development tool for mammalian perfusion culture. Biotechnol. Bioeng. 116, 1315–1325.
Tripathi, N.K., Shrivastava, A., 2019. Recent developments in bioprocessing of recombinant proteins: expression hosts and process development. Front Bioeng. Biotechnol. 7, 420.
Walsh, G., 2018. Biopharmaceutical benchmarks 2018. Nat. Biotechnol. 36, 1136–1145.
Zhang, Y., Gao, Z., Li, Z., Derksen, J.J., 2017. Transitional flow in a Rushton turbine stirred tank. AIChE J. 63, 3610–3623.